Bouncing Motions of Liquid Drops between Tilted Parallel-Plate Electrodes

The paper reports on experimental and analytic studies on translational motions of liquid drops in an immiscible, dielectric liquid confined by a pair of tilted parallel-plate electrodes, across which a steady electric field is being applied. With an increase of the strength of the field, drops begin to bounce back and forth between the electrodes while falling down along the axis of tilt of the electrodes. The bouncing motions are found to be predictable with a reasonable accuracy by using a simple model constructed within the framework of conventional fluid mechanics and electrostatics.

T. Mochizuki
Y. H. Mori
Department of Mechanical Engineering
Keio University
Yokohama 223, Japan

N. Kaji
Division of Mechanical Engineering
Institute of Vocational and
Technical Education
Sagamihara 229, Japan

Introduction

Liquid drops subjected to an electric field can show various motions depending on its strength, frequency, direction relative to the gravity, etc., as well as on the properties of the liquids constituting the drops and the surrounding medium. Typical examples are deformation of the drops, steady or periodical, toroidal circulations inside and outside of each drop, and Coulombic-force-driven migrations of the drops. These motions may be useful as a means of enhancing heat and/or mass transfer between the drops and the medium (Mori and Kaji, 1987). In this paper we consider a particular class of electrically-driven drop motions that has a potential for an effective enhancement of heat and/or mass transfer.

Suppose a liquid drop released into a medium of a dielectric liquid confined by a pair of parallel-plate electrodes across which a steady electric field is applied. If the drop had a net charge and the field strength between the electrodes was high enough, the drop would migrate toward either electrode, being driven by the Coulomb force, resulting in a collision with the electrode. While making an electrical contact with the electrode, the drop newly acquires a charge of the same sign as the electrode, which results in the bouncing back of the drop toward the other electrode. Consequently, the drop will exhibit a continual bouncing motion between the electrodes. Kaji et al. (1982) proposed to utilize the bouncing motions of drops as described above for the purpose of enhancing heat and mass transfer to or from the drops. They investigated the motions of and heat transfer to each water drop buoying up in the medium of a denser silicone oil, which was confined by a pair of vertically-oriented parallel-plate electrodes. It was observed that each drop showed a zigzag trajectory, bouncing back and forth between the electrodes, because of superposition of the Coulomb force and the gravitational force which were normal and parallel to the electrodes, respectively. This resulted in a high translational velocity of the drop and consequently a significantly increased heat transfer coefficient, while the residence time of the drop in the medium with a given height altered little from that available under no electric field.

Subsequently, Kaji and Mori (1986) proposed to apply the above transfer enhancement scheme to particle drying processes. They observed bouncing motions of solid particles while falling down in the air bounded by a pair of electrode plates whose angle of tilt from the vertical was so variable that the longitudinal component of gravity could be extensively reduced. It was confirmed that, by applying a sufficiently high electric field and a rather large angle of tilt, we can get simultaneously a high translational velocity and an enormously lengthened residence time of each particle in the space between the electrodes with a specified length.

In the present study, we deal with such liquid-liquid systems that may simulate those used in direct contact heat exchangers or solvent extractors. Single liquid drops are released into the medium of an immiscible, weakly conducting liquid which is confined by a pair of parallel-plate electrodes. The tilt angle of the electrodes and the strength of a steady electric field applied across them are considered primary factors controlling the drop motion. The dependencies of drop motion on these factors have

Correspondence concerning this paper should be addressed to T. Mochizuki, c/o Dr. Y. H. Mori, Department of Mechanical Engineering, Keio University, Yokohama 223, Japan.

been studied experimentally. Some simple models to simulate the drop motion have also been contrived, and the predictions by the models are compared with the experimental observations to test the potential utilities of the models in designing practical liquid-liquid contactors.

Experimental Apparatus and Procedure

Figure 1 schematically shows the structure of a rectangular column with which water drop motions in silicone oil were studied extensively. The column was fabricated of transparent PMMA [poly(methyl methacrylate)] plates, together with a water jacket enclosing it. It was equipped with a nozzle assembly and a pair of brass-plate electrodes, 2-mm-thick and 70-mm-wide, and was almost filled with a dimethyl silicone oil [KF96 (10 cst) fluid prepared by Shin-etsu Chemical Co., Tokyo] whose temperature was held at 51 ± 0.9°C. The electrodes were parallel to each other over the length of 350 mm along the column axis which was either vertical or tilted by a finite angle θ. The spacing, l, between them was adjusted to 25 mm or 40 mm with the aid of PMMA struts placed at their sides.

One electrode at a lower position was grounded, while to the other a positive or negative potential ϕ was applied from a Spellman 30PN30 high-voltage direct-current power supply. It should be noted that the brass plates serving as the electrodes had been once baked in an electric furnace, while having been wetted with the same silicone oil used as the continuous-phase liquid in the experiments. Hence, their surfaces were kept so hydrophobic that water drops do not get attached to them. The nozzle was made of a 27-gauge stainless-steel tube (0.41 mm OD and 0.20 mm ID) having a tip cut at right angles to its axis. It was always oriented vertically with its tip facing downward and was sheathed in a coaxial copper tube (10 mm OD and 8 mm ID) which extended 15 mm ahead of the nozzle tip. The nozzle and the copper tube were grounded simultaneously, and thus the copper tube could well shield the nozzle from an external electric field (Mori et al., 1987).

In fact, by feeding water (deionized and distilled) to the nozzle at a constant rate with the aid of a syringe infusion pump, we could release water drops of the same size into the medium of silicone oil irrespective of the strength of electric field applied across the electrodes. The equivalent spherical diameter D_o of drops was observed to be 4.91 ± 0.01 mm when the inside of the copper tube was filled with the silicone oil. The diameter could be reduced to 2.47 ± 0.01 mm, when air was kept in the tube so that drops were formed in the air, dripped onto the meniscus of silicone oil in the tube, and then released into the bulk of silicone oil.

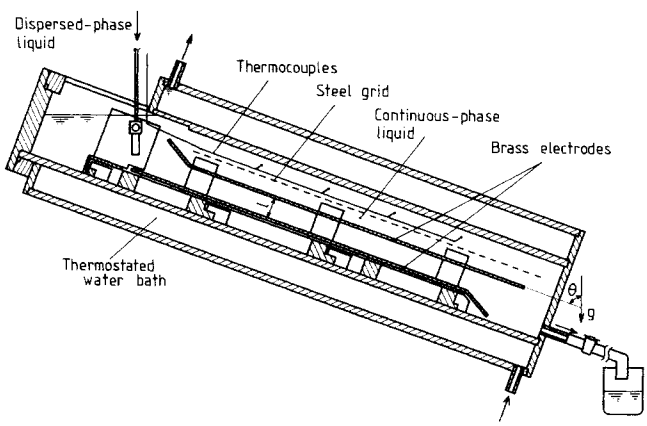

Figure 1. Test column structure used for the motions of water drops in silicone oil.

The column was rigidly fixed to a steel frame, whose tilt angle could be changed arbitrarily. The tilt angle of the column axis, θ, measured from the vertical was varied from 0° to 73.3°. The motion of each drop during its pass through the region between 186 and 246 mm down, along the column axis, from the entrance of the "parallel electrode section" was photographically recorded with a Locam Model-51 16-mm cinecamera, which slid down, following the drop, on a roller conveyor set parallel to the column.

Beside the test column illustrated above, we also used another apparatus in a supplementary experiment for comparing water drop motions in some different liquid media. In a PMMA-made flat cell, a pair of parallel brass-plate electrodes, each 2-mm-thick and 80-mm-square, were set horizontally leaving 25 mm spacing between them. A positive potential was applied to the upper electrode, while the lower one was grounded. The surfaces of the electrodes were made hydrophobic in the same way as explained above. Tested as the continuous-phase liquid to fill up the electrode spacing were the dimethyl silicone oil KF96 (10 cst), *n*-heptane, and a perfluorocarbon, FC-75 fluid prepared by Sumitomo-3M Co., Tokyo. The liquid temperature was always controlled to 25.8 ± 0.2°C. Physical properties, of the liquids used, possibly relevant to the drop motions, are listed in Table 1.

Experimental Observations

Whenever θ was finite and E_n, the nominal field strength given by $|\phi|/l$, was sufficiently low, drops simply slid and/or rolled down on the surface of the lower electrode. As E_n was increased beyond a certain threshold, which was dependent on θ, drops were levitated from the electrode surface after sliding some distance on it. When E_n was in excess of the threshold only slightly, drops, once levitated, were drifted down almost in parallel with the surface of either electrode. A further increase in E_n resulted in a migration of drops once levitated toward the upper electrode, making contact with it. The contact of each drop with the upper electrode was succeeded by an immediate repulsion of the drop toward the lower electrode, and thus the drop began to make a continuous bouncing motion between the two electrodes. Figure 2 exemplifies the trajectory of a drop making an apparently steady bouncing motion. An excessive increase in E_n caused a disintegration of each drop at the instant that the drop impinged on either electrode.

Indicated in Figure 2 are Λ and Λ_x, the length of travel and the axial displacement of the center of mass of each drop while the drop makes a round trip between the electrodes. Dividing Λ and Λ_x with the time spent in the round trip, we can deduce the mean translational velocity, $\overline{v}_t$, and the mean axial velocity, $\overline{v}_x$, of the drop. Later in this paper, drop motions are evaluated in terms of $\overline{v}_t$ and $\overline{v}_x$.

Theoretical Analysis

Here we present a simple analysis of such a bouncing motion of a drop. The predictions based on the analysis and relevant experimental results are discussed in the subsequent section.

Table 1. Physical Properties of the Liquids Used

	ρ kg/m^3	ν mm^2/s	σ against Water, mN/m	ϵ pF/m	χ $\Omega \cdot$ m
Water (51°C)	988[a]	0.553(50°C)[a]		616[b]	5.3×10^4(50°C)[a]
KF96 (51°C)	902[c]	6.69[d]	44.6[e]	21.8[f]	4×10^{12} [f]
Water (25°C)	997[g]	0.891[h]		693[b]	1.5×10^5(26°C)[a]
KF96 (25°C)	932[i]	10[i]		23.0[i]	$\geq 1 \times 10^{12}$ [i]
n-Heptane (25°C)	680[h]	0.582[g]	50.8[j]	17.1[a]	1.5×10^{11}(20°C)[a]
FC-75 (25°C)	1,760[i]	0.8[i]		16.4[i]	8×10^{13} [i]

[a]From *Landolt-Börnstein Data Book* (1955, 1959, 1960)
[b]From Malmberg and Maryott (1956)
[c]Measured with a pycnometer
[d]Measured with a glass capillary viscometer
[e]Measured by the pendant drop method
[f]Measured with the apparatus and procedure described by Kaji (1980)
[g]From *TRC Thermodynamic Tables* (1989)
[h]From *JSME Data Book* (1983)
[i]Manufacturer's data
[j]From Aveyard and Haydon (1965)

We assume a drop to be an electrically-conducting sphere which is suspended in a perfect dielectric medium and is subjected to a uniform electric field and gravity (Figure 3). The force balance on the drop may be written as

$$\frac{1}{6}\pi D^3(\rho_d + \frac{1}{2}\rho_c)\frac{d\boldsymbol{v}}{dt} = \frac{1}{6}\pi D^3(\rho_d - \rho_c)\boldsymbol{g} + Q\boldsymbol{E} - \boldsymbol{F}_D \quad (1)$$

In Eq. 1, the virtual mass of the drop is approximated by that for a steady translation of a sphere in an inviscid fluid of an infinite extent. The electric field is assumed to exert on the drop only a Coulombic force, $Q\boldsymbol{E}$. The net charge on the drop, Q, is evaluated to be a charge that a conducting sphere of diameter D would have when in contact at equilibrium with a conducting plane (electrode surface). That is given by (Félici, 1966)

$$Q = \tfrac{1}{6}\pi^3 \epsilon_c D^2 |\boldsymbol{E}| \quad (2)$$

The drag on the drop, $\boldsymbol{F}_D$, may be expressed as

$$\boldsymbol{F}_D = \tfrac{1}{8}\pi \rho_c C_D D^2 |\boldsymbol{v}| \boldsymbol{v} \quad (3)$$

Here we further assume that the instantaneous drag coefficient C_D is uniquely related to the instantaneous Reynolds number Re in just the same manner as the standard C_D—Re relation for steady motion of a sphere. The C_D—Re relation is formulated being based on either "rigid sphere approximation" or "fluid sphere approximation." In the former, the drop surface is supposed to be rigid because of an adsorption of a considerable amount of surface-active contaminants. In the latter, the drop surface is assumed to be clean and hence it does not provide any resistance to the viscous shear acting from the medium. The correlations we employed for selective use in our calculation are listed in Appendix 1.

In solving Eq. 1, with the aid of Eqs. 2 and 3, and the C_D—Re relations, we must specify the mechanical condition of drop/

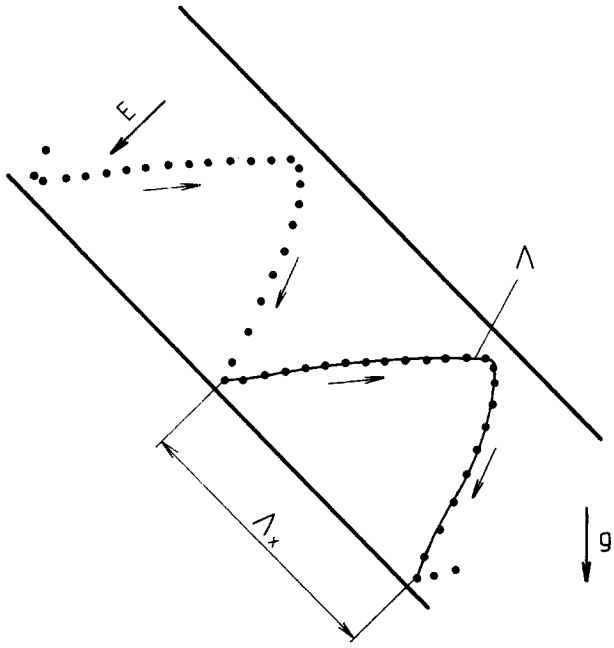

Figure 2. Trajectory of a water drop making a bouncing motion in silicone oil.

$l = 25$ mm, $D_o = 4.91$ mm, $\theta = 45.5°$, $E_a = 0.15$ MV/m.
Dots show instantaneous locations of the center of mass of the drop. Λ and Λx denote the length of travel and the axial displacement of the center of mass of each drop while the drop makes a round trip between the electrodes.

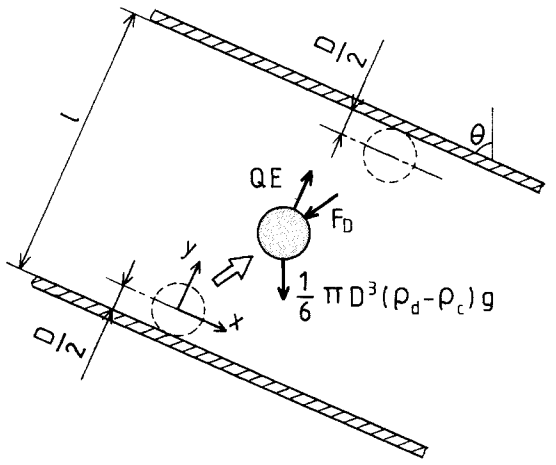

Figure 3. Force balance on an electrically-conducting sphere between a pair of parallel-plate electrodes.

electrode collision. We assume a perfectly inelastic collision that causes no initial y component of velocity $\boldsymbol{v}$ of a drop departing from the electrode surface. Concerning x component of $\boldsymbol{v}$, we assume one of the following conditions:

1. *Stick Condition.* At each collision with electrode surface, a drop completely loses its momentum and "sticks" on the surface.

2. *Slip Condition.* A drop completely loses its y momentum, but suffers no frictional loss in its x momentum. (The "slip condition" does not mean that x momentum is preserved at each contact of a drop with electrode surface, because a drastic reduction in magnitude of $\boldsymbol{v}$ at the contact causes a significant increase in C_D, which in turn results in a reduction in v_x.)

In any collision in a real system, there must exist a finite "effective" coefficient of restitution, because of a finite drop/medium interfacial tension and a finite friction coefficient at the drop/electrode interface. Thus, either of the two conditions stated above represents an extreme case. It turns out that for each operational condition characterized by l, D_o, θ and E_n, four different solutions are available depending on the combination of the "rigid and fluid sphere approximations" and the "stick and slip conditions."

Equation 1 was integrated numerically, using the initial condition:

$$t = 0; \qquad y = D/2, \qquad v_x = v_y = 0 \tag{4}$$

The number of time increments we set for computing each round trip of a drop, in which y changes from $D/2$ to $\ell - D/2$ and then back to $D/2$, was over 4.5×10^4. (Reducing the number of time increments to a half resulted only in a change of solution by well below 1%.) When the "stick condition" was employed, the computation was accomplished by following one round trip. When the condition is replaced by the "slip condition," the computation was continued over many round trips till Λ_x (Figure 2) obtained for the last round trip agree with that obtained in the preceding trip within 1%.

Experimental vs. Theoretical Results

In the following, both experimental and theoretical results are shown exclusively in the form of $\bar{v}_t/v_o$ and $\bar{v}_x/v_o$ vs. E_n or θ, where v_o means the terminal velocity of drops to be available in the presence of gravitational field only. The values of v_o determined experimentally are given in Table 2 for comparison with those predicted from the standard C_D—Re correlations in Appendix 1. The experimental results given in Figures 4 to 8 are those obtained exclusively with positive potentials applied to the upper electrode. A possible effect of the change in the polarity of the electrode is discussed later.

Table 2. Terminal Velocities of Drops

	D_o mm	v_o, mm/s Experimental	Rigid-Sphere Approx.	Fluid-Sphere Approx.
Water/KF96 (51°C)	4.91	66.8 ± 0.0	59.9	100
Water/KF96 (51°C)	2.46	28.7 ± 0.2	26.5	38.7
Water/KF96 (25.8°C)	4.69	42.1 ± 0.3	38.4	
Water/*n*-heptane (25.8°C)	2.45	164 ± 5	171	
Water/FC-75 (25.8°C)	2.61	144 ± 5	165	

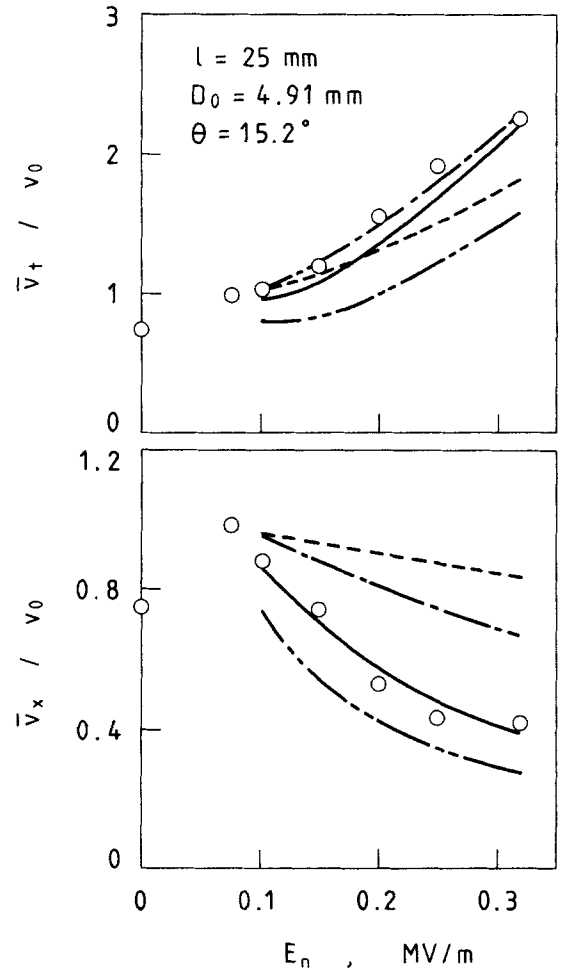

Figure 4. Theoretical predictions vs. experimental results for the case of l = 25 mm, D_o = 4.91 mm, and θ = 15.2°.

O = experimental; ——— = rigid sphere approximation/stick condition; —·— = rigid sphere approximation/slip condition; – – – = fluid sphere approximation/stick condition; ------- = fluid sphere approximation/slip condition.

Four classes of solutions, which depend on the selection of drop-surface mobility approximations and drop/electrode collision assumptions combined with Eq. 1, were obtained for a specific operational condition and compared with corresponding experimental results. It is shown in Figure 4. For the uncertainty of each experimental data point, refer to Appendix 2. The lefthand side of each curve representing a particular class of solutions corresponds to the critical field strength, below which continual bouncing motion of drops was no longer observed in the experiments. This is also the same in Figures 5 to 8.

Figure 4 shows that the solutions based on the "rigid sphere approximation" and the "stick condition" agree most with the experimental results overall. Therefore, only the solutions of this class are shown in Figures 5 to 8 for comparison with corresponding experimental results.

In Figure 5 we find, as expected, that at any tilt angle θ, $\bar{v}_t$ sharply increases with an increase in E_n while $\bar{v}_x$ decreases

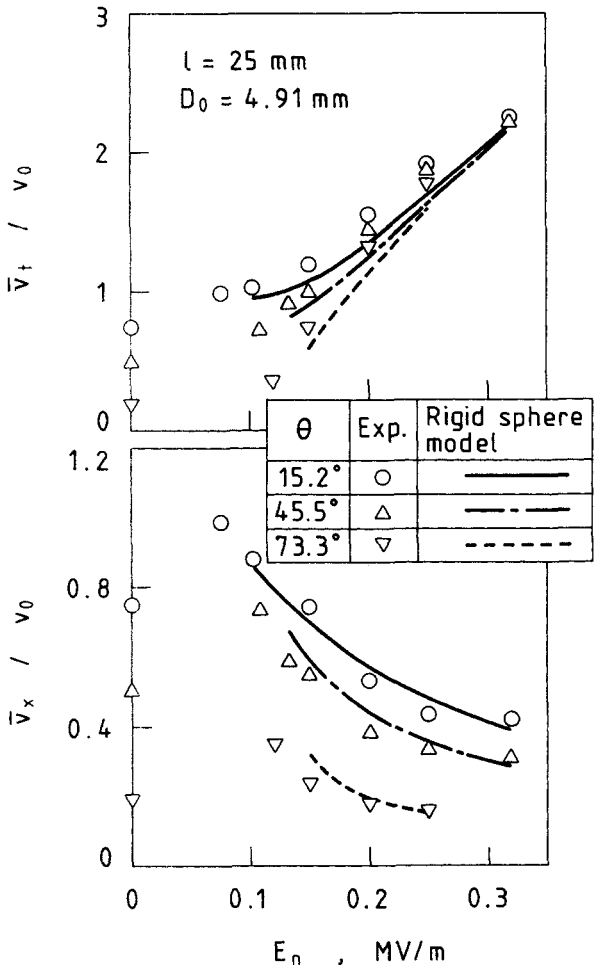

Figure 5. Dependencies of mean translational velocity, $\bar{v}_t$, and mean axial velocity, $\bar{v}_x$, of water drops (D_o = 4.91 mm), on field strength when l = 25 mm.

v_o means the terminal velocity of drops of the same size.
Curves represent theoretical predictions based on "rigid sphere approximation" and "stick condition."

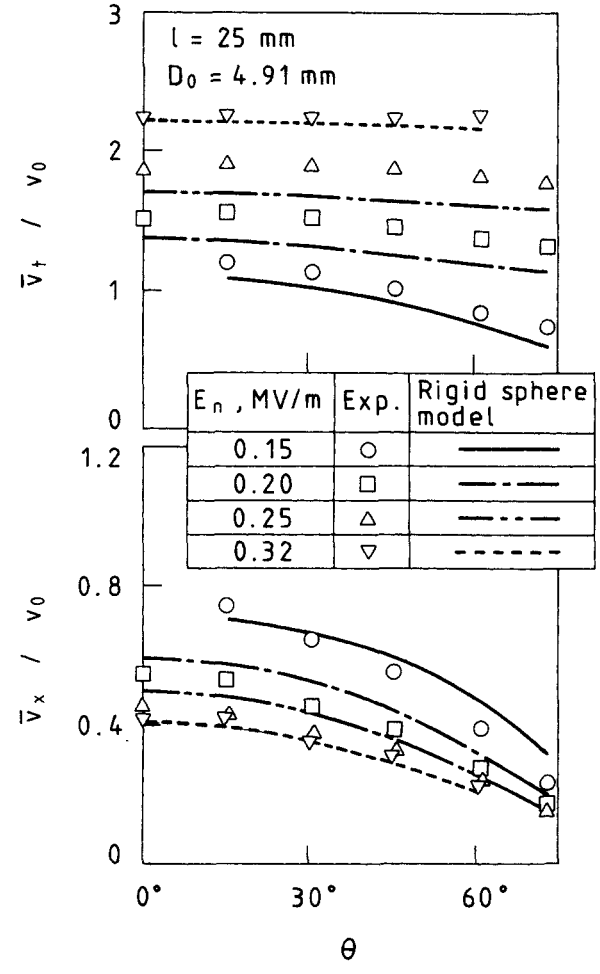

Figure 6. Dependencies of $\bar{v}_t$ and $\bar{v}_x$ on tilt angle of the electrodes, l = 25 mm, Do = 4.91 mm.

asymptotically to a constant level. Figure 6 demonstrates how $\bar{v}_x$ is reduced by increasing θ without retarding $\bar{v}_t$ (except in a lower range of E_n). It becomes evident that for drops of ~4.91 mm in D_o, $\bar{v}_t$ can be increased to about 2.3 times as large as v_o, without inducing drop disintegration, and that $\bar{v}_x$ can be lowered to 0.15 times v_o by increasing θ to 73.3°.

Figure 7 represents three sets of results: two of them were obtained under the same condition except for a difference in l or D_o. We note that the drop motion does not alter so largely with the variation of l. We also find that smaller drops exhibit a larger increase in $\bar{v}_t/v_o$ with an increase in E_n than larger drops do. In contrast, little difference depending on the drop size is recognized in the variation of $\bar{v}_x/v_o$ with E_n.

A possible effect of the direction of electric fields was tested by changing the sign of ϕ, the voltage applied to the upper electrode. The strength of electric field in a dielectric liquid is, in general, not constant over the whole spacing between the electrodes because of the presence of space charge. The distribution of the field strengths across the spacing can be significantly asymmetric (Foster, 1962; Kaji et al., 1982). Whenever the distribution of the field strengths is asymmetric, the reversal of the field direction will cause a change in the history of the resultant force (the Coulombic force plus the gravity) to affect each drop during its round trip between the electrodes, possibly resulting in a change in its translational motion. Nevertheless, we did not find any appreciable change either in $\bar{v}_t$ or in $\bar{v}_x$ when the direction of the field was reversed in the experimental system.

Figure 8 summarizes the drop motions observed in the apparatus which has a pair of parallel-plate electrodes set horizontally. A bouncing motion has been confirmed to occur in the medium of *n*-heptane and FC-75 as well. In terms of quality, no significant difference in drop behavior was noted when changing the medium liquid from silicone oil to *n*-heptane or FC-75 in spite of appreciable differences in physical properties of the three liquids (see Table 1).

We note that theoretical predictions represent with a reasonable accuracy the general dependencies of drop motions on operational parameters such as l, D_o, and E_n (Figures 5 to 8). Considerable deviations of predictions from the experimental results are noted, however, at higher field strengths applied to *n*-heptane and FC-75. The deviations are possibly ascribable to

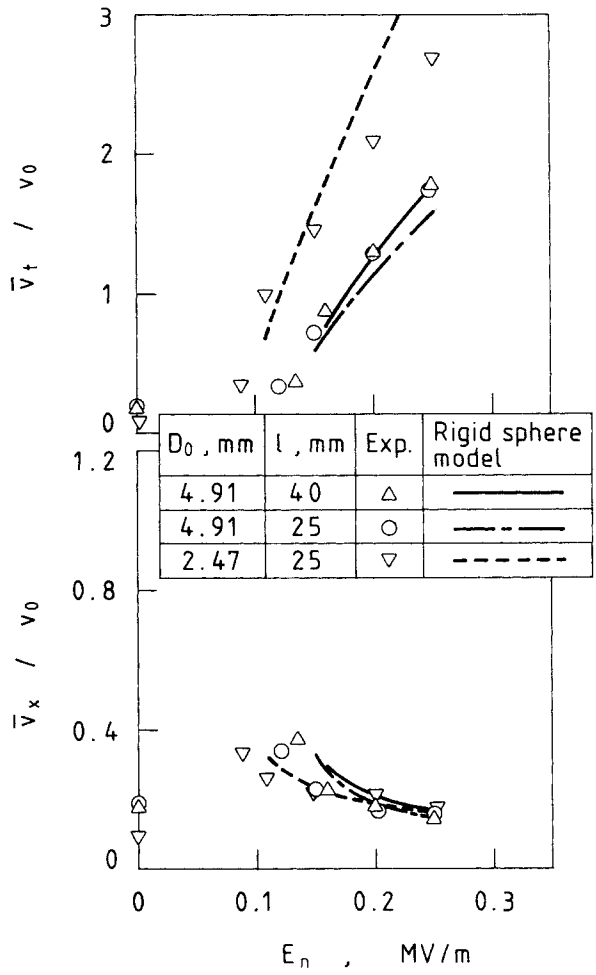

Figure 7. Dependencies of $\bar{v}_t$ and $\bar{v}_x$ on the spacing between the electrodes, l, and on the drop diameter, D_0.

$\theta = 73.3°$.

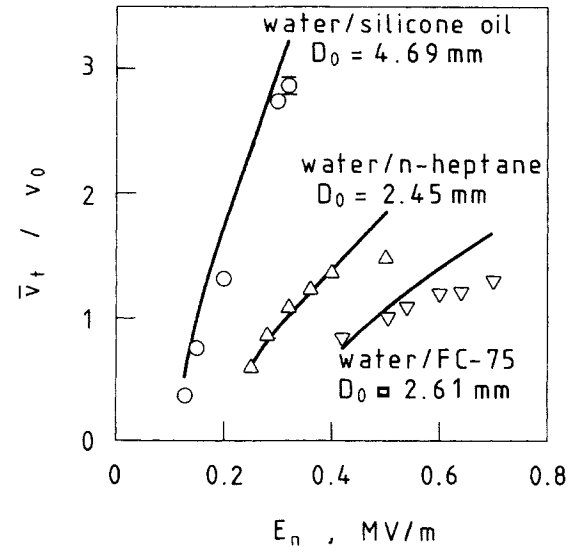

Figure 8. Dependencies of $\bar{v}_t$ on E_n in the three systems: water/silicone oil, water/n-heptane, and water/FC-75.

the evaluation of Q by Eq. 2, deformation and oscillation of drops causing variations in drag, an interaction of each drop with its own wake when rebounding from electrode surface, etc.

Acknowledgment

We are indebted to Dr. Y. Tochitani of Kanazawa Institute of Technology, Dr. K. Uematsu and Dr. A. Watanabe of Keio University, for their advice on the measurements of the physical properties of the test fluids. We are also grateful to Y. Ishikubo, T. Asano, and T. Hasegawa, students at the Department of Mechanical Engineering, Keio University, for their assistance in the experiments and data analyses.

Notation

C_D = drag coefficient
D, D_o = diameter of electrically conducting sphere and equivalent spherical diameter of liquid drop
E, E_n = electric field and its nominal magnitude
F_D = drag on drop
g = acceleration of gravity
l = spacing between parallel-plate electrodes
Q = net electric charge on drop
Re = Reynolds number, $D|v|/\nu_c$
v = instantaneous velocity of electrically conducting sphere
v_t, v_x = translational and axial velocities
$\bar{v}_t, \bar{v}_x$ = mean of v_t and v_x
v_o = terminal velocity of drop
w = $\log_{10} Re$
x, y = coordinates defined in Figure 3

Greek letters

ϵ = electrical permittivity
θ = tilt angle of column axis from vertical
κ = drop-to-medium viscosity ratio
Λ, Λ_x = trajectory length of the center of drop mass and axial displacement during its round trip between electrodes
ν = kinematic viscosity
ρ = mass density
σ = interfacial tension
ϕ = electric potential or voltage difference between electrodes
χ = electric resistivity

Subscripts

c, d = medium liquid and drop

Literature Cited

ASME, "Measurement Uncertainty—ANSI/ASME PTC19.1–1985," *Performance Test Codes, Supplement on Instruments and Apparatus*, Part 1 (1986).

Aveyard, R., and D. A. Haydon, "Thermodynamic Properties of Aliphatic Hydrocarbon/Water Interfaces," *Trans. Farad. Soc.*, **61**, 2255 (1965).

Clift, R., J. R. Grace, and M. E. Weber, *Bubbles, Drops, and Particles*, Academic Press, New York (1978).

Félici, N.-J., "Forces et Changes de Petits Objets en Contact avec une Électrode Affectée d'un Champ Électrique," *Revue Générale de L'Électricite*, **75**, 1145 (1966).

Foster, E. O., "Electric Conduction in Liquid Hydrocarbons. I. Benzene," *J. Chem. Phys.*, **37**, 1021 (1962).

Hamielec, A. E., and A. I. Johnson, "Viscous Flow Around Fluid Spheres at Intermediate Reynolds Numbers," *Can. J. Chem. Eng.*, **40**, 41 (1962).

Hamielec, A. E., S. H. Storey, and J. M. Whitehead, "Viscous Flow Around Fluid spheres at Intermediate Reynolds Numbers (II)," *Can. J. Chem. Eng.*, **41**, 246 (1963).

JSME Data Book: Themophysical Properties of Fluids, JSME, Tokyo, Japan (1983).

Kaji, N., "Direct-Contact Heat Transfer to Drops in an Intermittent Electric Field," D. Eng. Thesis, Keio University, Yokohama, Japan (1980).
Kaji, N., and Y. H. Mori, "Bouncing Motions of Drops and Particles between Parallel-Plate Electrodes—A Preliminary Study of Drying Augmentation," *Drying '86*, A.S. Mujumdar, ed., Hemisphere, Washington, DC, **2**, 819 (1986).
Kaji, N., Y. H. Mori, Y. Tochitani, and K. Komotori, "Electrohydrodynamic Augmentation of Direct Contact Heat Transfer to Drops Passing Through an Immiscible Dielectric Liquid: Effect of Field-Induced Shuttle Migration Between Parallel-Plate Electrodes of Drops," *Proc. Int. Heat Transfer Conf.*, **5**, 231 (1982).
Landolt-Börnstein Zahlenwerte und Funktionen aus Physik, Chemie, Astronomie, Geophysik und Technik, II-6, II-7, and IV-1, Springer-Verlag, Berlin, West Germany (1955, 1959, 1960).
Malmberg, C. G., and A. A. Maryott, "Dielectric Constant of Water from 0° to 100°C," *J. Res. Nat. Bureau Standards*, **56**(1), 1 (1956).
Mori, Y. H., and N. Kaji, "Enhancement of Heat or Mass Exchange between Drops and a Medium Through Application of Electric Field," *Heat Transfer in High Technology and Power Engineering*, W.-J. Yang and Y. Mori, eds., Hemisphere, Washington, DC, 380 (1987).
Mori, Y. H., M. Ichikawa, and N. Kaji, "An Attempt at Applying an Electric Field for Enhancing Direct Liquid/Liquid Contact Heat Exchange in a Spray Column: Formation and Release of Drops in Electric Fields," *Proc. ASME · JSME Therm. Eng. Joint Conf.*, **3**, 19 (1987).
TRC Thermodynamic Tables, Thermodynamics Research Center, Texas A&M University System, College Station (1989).

Appendix 1: C_D—Re Relations Used in Numerical Calculations

The mathematical C_D—Re relations we employed in solving Eq. 1 are:

For Rigid Sphere Approximation:

$$C_D = \frac{3}{16} + \frac{24}{Re} \qquad (Re < 0.01) \quad \text{(A1)}$$

$$C_D = \frac{24}{Re}\left[1 + 0.1315\, Re^{(0.82 - 0.05\, w)}\right] \qquad (0.01 \leq Re \leq 20) \quad \text{(A2)}$$

$$C_D = \frac{24}{Re}\left[1 + 0.1935\, Re^{0.6305}\right] \qquad (20 \leq Re \leq 260) \quad \text{(A3)}$$

$$C_D = 10^{(1.6435 \,-\, 1.1242\, w \,+\, 0.1558\, w^2)} \qquad (260 \leq Re \leq 1{,}500) \quad \text{(A4)}$$

where

$$w = \log_{10} Re$$

For Fluid Sphere Approximation:

$$C_D = \frac{8}{Re}\left(\frac{2 + 3\,\kappa}{1 + \kappa}\right) \qquad (Re \leq 0.4) \quad \text{(A5)}$$

$$C_D = \frac{3.05\,(783\,\kappa^2 + 2142\,\kappa + 1{,}080)}{(60 + 29\,\kappa)\,(4 + 3\,\kappa)\,Re} \times \left[1 + \exp(-1.72 + 0.21w + 0.036w^2 - 0.0041w^3)\right] \qquad (0.005 \leq \kappa \leq 0.19, \quad 0.4 \leq Re \leq 10) \quad \text{(A6)}$$

$$C_D = \frac{3.05\,(783\,\kappa^2 + 2142\,\kappa + 1{,}080)}{(60 + 29\,\kappa)\,(4 + 3\,\kappa)}\, Re^{-0.74} \qquad (10 \leq Re) \quad \text{(A7)}$$

where κ is the drop-to-medium viscosity ratio.

Equations A1–A4 are recommended by Clift et al. (1978). Equation A5 is the so-called Hadamard-Rybczynski solution (Clift et al., 1978), and Eq. A7 is attributed to Hamielec et al. (1962, 1963). We correlated Eq. A6 so that C_D and its first derivative with Re predicted by the correlation agree with those given by Eq. A5 at $Re = 0.4$ and with those by Eq. A7 at $Re = 10$ within ±2%.

Appendix 2: Experimental Uncertainty

Each data point in Figures 4 to 8 represents the arithmetic mean of 3 to 15 independent data, obtained successively in the same series of experiments, on the variable taken on the ordinate ($\bar{v}_t/v_o$ or $\bar{v}_x/v_o$). The uncertainty of the mean at ~95% coverage has been evaluated, according to the standard uncertainty-analysis procedure (ANSI/ASME, 1986), assuming the data to be free from any bias error. The magnitude of the uncertainty thus evaluated is indicated by a vertical bar skewering the data point only when the former exceeds the dimension of the latter.

However, the uncertainty can increase even further. The hydrophobicity of the electrode surfaces depended on the "electrode baking" procedure that preceded each series of experiments. The largest deviations in $\bar{v}_t$ and $\bar{v}_x$ found while repeating the electrode baking procedure were ~30% and ~18%, respectively.

Manuscripts received Jan. 16, 1990, and revision received Apr. 20, 1990.